Comparing Two Field Methods to Measure Individual Shrubs' Root Density Distribution and Establish Allometric Equations for Belowground Biomass

Ciro Cabal (ccabal@princeton.edu)
Princeton University https://orcid.org/0000-0002-7222-1991
Laura Rodríguez Torres
Neus Marí-Mena
Antonio Más Barreiro
Antón Vizcaíno
Joaquin Vierna
Fernando Valladares
Stephen W Pacala

Research Article

Keywords: Microsatellite, Plant injection, Core drilling, Plant allometry, Root foraging behavior, Crown biovolume

Posted Date: February 7th, 2022

DOI: https://doi.org/10.21203/rs.3.rs-1307570/v1

Abstract

Purpose: A large fraction of a plant's biomass is thought to be belowground, especially in shrublands that typically occur in episodically water-limited climates. Nonetheless, we have no standardized method to map individual plant's root density distribution (IRDD) and lack of easily obtainable allometric predictors of shrubland belowground biomass. This type of information is difficult to collect, especially in woody plant communities in natural conditions where roots of different individuals can be highly intermingled.

Methods: We assess three methods to map IRDD of field shrubs: soil drilling to extract roots, and plant injection with dyes and microsatellite analysis for individual-level root identification. Using the resulting data, we fitted IRDD models and integrated root density predictions from the models across three-dimensional space obtaining total root biomass of shrubs. We use the resulting individual-level data to establish allometric relations based on two easy-to-measure predictors: crown biovolume and stem diameter at the ground level.

Results: We found plant injection to be a highly cost-effective technique to link root fragments from a soil sample to plant individuals. We fitted power law distributions predicting aboveground and belowground biomass.

Conclusions: Core drilling machines and plant injection with dyes of different colors to link root fragments from the sample pool to plant individuals represent an affordable, reliable way to study the foraging behavior of woody plants which roots are highly intermingled. The resulting allometric relations allowed us to conclude that crown biovolume is the best proxy for shrub biomass, especially belowground.

1 Introduction

Shrublands cover about 7-8% of Earth's land surface (Lal, 2004; Maestre et al., 2021), and are increasing because of anthropogenic desertification (Eldridge et al., 2011; Huang et al., 2020). Shrubs are an important functional type of vegetation amid largely undervalued by humankind (Tomaselli, 1977; Kemper, Cowling, & Richardson, 1999) and understudied by ecologists, as compared to forest and grassland systems (Wullschleger et al., 2014; Fusco, Rau, Falkowski, Filippelli, & Bradley, 2019; Schrader-Patton & Underwood, 2021). Shrubs grow in resource-poor soils, and allocate much of their biomass to their roots to acquire water and soluble nutrients (Schenk & Jackson, 2002; Bardgett, Mommer, & De Vries, 2014). Through their roots, they absorb and compete for water, nitrogen, phosphorus, and many other soil resources that are subsequently transported to the leaves where plants need them to photosynthesize (Lambers et al. 2008; Kirkham, 2014). However, compared to aboveground plant organs, we know very little about roots, since roots cannot be directly observed and are very difficult to measure (Jones et al., 2011; Lux & Rost, 2012). Additionally, most of what we know about plant roots come from experiments conducted in controlled conditions, yet rooting behavior of plants may be very different in the wild

(Poorter et al., 2016). Developing, testing, and standardizing methodologies to measure root traits in the field is a salient pending task for ecologists to address (Addo-Danso, Prescott, & Smith, 2016).

Allometric relationships provide estimates of ecosystem-level above- and belowground biomass from non-destructive and time-efficient biometric measurements, and are very common in forestry science, especially for species with commercial value (Wirth, Schumacher, & Schulze, 2004; Muukkonen, 2007; Chen, Hobbie, Reich, Yang, & Robinson, 2019). Allometric relationships have proven very useful to scale processes from the individual to the landscape in global vegetation models (Tyree & Ewers, 1991; Fischer, Maréchaux, & Chave, 2019). While some shrub allometries from temperate (Smith & Brand, 1983), mediterranean (Usó, Mateu, Karjalainen, & Salvador, 1997), desert (Allen, Pockman, Restrepo, & Milne, 2008; Ma & Wang, 2021), and alpine (Elzein, Blarquez, Gauthier, & Carcaillet, 2011) biomes have been published, they are much less common than published tree allometries (He et al., 2018). Tree allometric relations are usually established using the diameter of the trunk at breast height (dbh, around 1.30 meters)—an easy biometric that has been proven to correlate well with other plant-level variables (Hamilton, 1975; O'Brien et al., 1995; Drexhage & Colin, 2001). However, shrub allometries cannot be based on a metric like dbh, because shrubs are by definition multi-stemmed.

Establishing specific allometric equations for belowground biomass requires obtaining and analyzing direct root measures in the first place. While many root variables can be measured (Freschet, Pagès, et al., 2021; Freschet, Roumet, et al., 2021), the individual-level root density distributions (IRDD) would provide the most comprehensive ecological information about plant foraging strategies (Cabal, De Deurwaerder, & Matesanz, 2021). IRDD maps allow researchers to study both the root density distribution of neighboring plants in the soil and, by integration of such densities in three-dimensional space, the plant allocation of biomass to belowground tissues (Cabal, Martínez-García, De Castro Aguilar, Valladares, & Pacala, 2020). Estimating an IRDD would require samples of roots from known spatial coordinates and depths, which can be accomplished with a core drill, and the assignment of roots in the sample to the surrounding individual plants (Cabal et al., 2021). A few studies have used microsatellite analyses to link root samples to individual plants (Brunner, Brodbeck, Büchler, & Sperisen, 2001; Saari, Campbell, Russell, Alexander, & Anderson, 2005; Lang, Dolynska, Finkeldey, & Polle, 2010). However, dying plant roots with different colors by injecting dye into their above ground stems might be a cheaper and easier alternative to DNA analysis. This technique has been used successfully in several experiments in controlled conditions, in plants grown in pots in the greenhouse (Murakami et al., 2006; Cahill et al., 2010; Cabal et al., 2020) and in tomato plants grown in outdoor containers (Murakami et al., 2011), but has never been used in woody plants in the field.

In this study, we first evaluate three field methods to map IRDD in three mediterranean shrub species growing in central Spain. Firstly, as a method for root extraction, we adapted a diamond core-drilling engine designed for the construction industry. Secondly, we compared two different root identification methods to link root fragments from soil samples to aboveground plants: microsatellite analyses and plant injection with dyes. Based on the results, we estimated root allometries for each species and

compared the success of stem diameter at the ground level and aboveground biovolume as allometric predictors.

2 Materials And Methods

For a detailed description of all our materials and methods, electronic supplementary materials are available. (*i*) Text and SM figures in "**Detailed Materials and Methods**" is an extended and detailed version of the Materials and Methods of this paper. (*ii*) The video documentary "**A Method for Identifying Shrub individual Root Density Distribution**" describes the study site, and the method combining core extraction using a construction diamond drill and root staining by plant injection. (*iii*) The "**Data and Code**" folder includes all the collected data and several R scripts (R Core Team, 2017) with all the code necessary to process the raw data, produce graphical outputs, and performe the statistical analyses. In the following, we present a summarized description of our methods.

2.1 Study site description

This study was carried out in a mediterranean shrubland in 'Las Tejoneras' (40º06'42.69" N, 5º16'32.46" W, 329 m.a.s.l.), Candeleda (Ávila, Spain), a small isolated granitic mountain that rises about 50m above the surrounding plains. It is dominated by leptosols and superficial bedrock. The area presents a meso-mediterranean, sub-humid ombroclimate (Rivas-Matínez & Armaiz, 1984) with characteristic arid summers, an annual precipitation of 797.9 mm, and a mean temperature of 16.17 ºC during the last decade (from January 2010 to December 2019 data from the AEMET meteorological station in Candeleda, 40°08'21" N, 5°18'41" W, 350 m.a.s.l.). The vegetation growing in this terrain is a biodiverse mediterranean closed-canopy shrubland with over a dozen shrub species. Three dominant shrub species were selected: gum rockrose (*Cistus ladanifer* L.), rosemary (*Salvia rosmarinus* Schleid.), and hairy-fruited broom (*Cytisus striatus* [Hill] Rothm).

2.2 Field data collection

Seven 2 x 2 meter plots were selected based in the occurrence of individuals of the targeted species and in order to represent a range of plant sizes within each species from small to the largest in the region. One monospecific rosemary plot was sampled in the summer of 2018, with 14 plants whose roots were identified using microsatellite markers developed by Segarra-Moragues & Gleiser (2009). Six plots were sampled in the summer of 2019, with seven rosemary, 11 rockrose, and six broom plants of different sizes, whose roots were identified by root injection with dyes. In the later six plots, a maximum of five focal individuals per plot were selected given that we used five different dye colors. Selected focal plants from each plot were measured to record their crown height, stem diameter at the ground level, hardwood area, age (annual rings), crown area, and total dry weight of photosynthetic and structural aboveground biomass. We calculated the crown biovolume of focal shrubs multiplying the crown height by the crown area, which we considered to be the best geometrical approximation to individuals' crown shape in our closed-canopy shrubland.

Subsequently, we extracted soil cores of a maximum depth of 800 mm and diameter of 104 mm with a core drilling machine designed for construction, and adapted to the field (**Fig SM 1-3**). Several cores were extracted from each plot following a regular spatial pattern. Several soil samples were obtained from each core at different depths. Soil samples were sifted using a 2 mm sieve, recovering mineral material (gravel and stones) whose volume was measured, and large root fragments whose diameter and dry weight was measured. Organic matter from the fraction of sample that passed through the sieve was recovered by flotation. Such organic matter was oven dried, we separated the fine roots—all with mean diameter <0.5 mm—from other materials, and weighed these roots in bulk.

The relative location of the insertion points of the stem of each focal plant to the soil surface (plant insertion) and the centroid of each cylinder-shaped soil sample (sample centroid) in the plot were located in three-dimensional space. To that end, we used a combination of drone photography, laser level measurements of the slope in the plot, and information about the minimum and maximum depth of each soil sample (**Fig SM 4-5**).

For gum rockrose and rosemary, we also measured the reproduction allocation and aboveground tissue turnover rates. To that end, we selected several individuals of different sizes in the study site and collected the litter they produced over the course of one year in trays of known surface area. We oven dried the plant litter, separated reproductive, photosynthetic, and structural tissues, and measured the dry weight of each fraction per plant.

2.3 Individual-level identification of roots

In the first plot, 14 leaf samples representing the plant individuals and 904 root fragments extracted from 42 soil samples from 23 soil cores were analyzed, linking roots to aboveground tissues using DNA analysis. Given the large number of collected root fragments, and the high per sample cost for DNA analysis, we only retained those root fragments having a diameter > 1 mm for the DNA analysis (415 root fragments). The selected roots were analyzed individually, following a dual approach. First, root DNA was isolated, and the region of the chloroplast ribulose-1,5-bisphosphate carboxylase/oxygenase large subunit (rbcL) gene was amplified by polymerase chain reaction (PCR) and sequenced. We compared the resulting sequences with barcode records available in two public reference databases to verify that the samples belonged to rosemary plants. Then, the roots with detectable rosemary barcodes (217 root fragments), together with the 14 leaf samples, were genotyped using six different microsatellite loci in four multiplex reactions.

In the six remaining plots, 24 plants were injected with dyes of different colors before soil coring. 2,840 root fragments were extracted from 216 soil samples in 81 soil cores and linked to the plants based on the dye colors (**Fig SM 6**). Because woody plants have never before been injected with dyes in order to link root fragments to plants, we developed a hydraulic model to estimate the velocity of dye in the stem vessels ($\vec{v_{10}}(f)$), as a function of the mean plant vessel diameter, the root length that the researcher wants to stain, the soil water potential, and the osmotic potential of the dyes used (**Fig SM 7**). We

obtained measures of the vessel diameter of the three focal species of our study and measured the osmotic potential of the dyes used with a psycrometer. The model assessment suggested a staining approach exerting 1.5 bar over a period of 30h. Other researchers aiming to use the plant injection method can use our model to estimate the pressure and time required in their own system. Root fragments were identified in the lab using two methods (**Fig SM 8**). First, we visually identified the color inside the roots under the bark. All roots for which color was not visible with the naked eye were introduced in a small plastic zip bag with water and kept at a constant temperature of 50 ºC in a water bath. Bags were checked after five minutes, two hours, and one day, to see if any colorant dissolved in the water. When a dye was detected in a root, either visually or in dissolution in water, the root was linked to the plant stained with the same color in the plot. Using cross-sectional cuts of the stained stems supports, besides assessment of hardwood area and plant age, the measurement of the sapwood area as this presents the actively transporting and therefore stained part of the stem (**Fig SM 9**).

2.4 Data processing

We calculated the Euclidian distance between every focal plant insertion and all soil sample centroids in the same plot, which allowed us to link data from the soil samples and plants. We sorted roots into diameter classes, differentiating fine (< 2 mm) and coarse roots (≥ 2 mm), and, within fine roots, diameters of: S (1.0 to 1.99 mm), XS (0.50 to 0.99 mm), and XXS (< 0.50 mm). For each soil sample, we calculated rooting volume (small mineral and organic particles and pores within) by subtracting the measured volume of gravel and stone from the total volume of the cylindrical sample, and root density was calculated as the root dry biomass (mg) per rooting volume (cm^3) of the soil sample. Root densities (RD) could thus be calculated for the various diameter classes and for each individual plant that was dyed or genetically analyzed, or for all roots collectively.

2.5 Data analysis

We fitted generalized linear mixed models to our data with plant individual as a random factor. All considered models predicted a plants' individual root density in every point of soil; hence, we called our models individual root density distribution (IRDD) models. We fitted independent models for each species, and for fine-roots (fIRDD) and coarse-roots (cIRDD). We designed the fIRDD models to account for the mechanisms of the plant foraging behavior of the exploitative segregation theory (Cabal et al., 2020). This assumed the following: (*i*) The self-root density distribution decreases quadratically with the distance from the plant to the point of soil, as the production and maintenance costs of transporting roots increase. (*ii*) Non-self-root density, i.e., the density of all roots in the same sample not linked to the focal individual (representing local belowground competition in each soil patch), can have negative or positive effects on the root density of the focal plant, both directly and through a statistic interaction with the Euclidian distance. This is because the exploitative segregation theory predicts that the effect of non-self-roots on self-root density is positive close to the focal plant stem, meaning that the plant will overproliferate roots, but that is negative far away from the plant stem, meaning that the plant will underproliferate and hence segregate its root system from others. (*iii*) That the size of the plant measured as aboveground dry biomass affects the root density. Finally, because resource concertation usually has

a heterogeneous vertical profile in soil, (*iv*) that the sample depth impacts plant root density. The cIRDD models simply predicted the coarse root density based in the fine root density (RD_f) predicted by the corresponding fIRDD in the same soil sample. We fitted eight independent IRDD models (Table 1).

Table 1
Full description of the eight independent IRDD models fitted in this study. Symbols: '*m*' method, 'M' Microsatellite, 'PI' Plant Injection, 'S' 1.0<Ø<1.99mm, 'E' Euclidian distance between plant stem and sample centroid, 'NSR' Non-self root density in the same soil sample, 'D' depth of soil sample centroid, 'AW' aboveground weight of the plant, 'E:NSR' interaction between E and NSR, 'Cl' rockrose *C. ladanifer*, 'Cs' broom *C. striatus*, and 'Sr' rosemary *S. rosmarinus*.

		Resp. var.	Fitted data			Explicative variables
Model			Meth.	Ø class	Species	(full model)
[1]	fIRDD+*m*	RD_{S+m}	*M+PI*	S	Rosemary	*E + NSR + E:NSR + D + AW + m*
[2]	cIRDD+*m*	RD_{c+m}	*M+PI*	coarse	Rosemary	RD_{S+m} *+ m*
[3]	fIRDD (Cs)	RD_{f-Cs}	*PI*	fine	Broom	*E + NSR + E:NSR + D + AW*
[4]	cIRDD (Cs)	RD_{c-Cs}	*PI*	coarse	Broom	RD_{f-Cs}
[5]	fIRDD (Cl)	RD_{f-Cl}	*PI*	fine	Rockrose	*E + NSR + E:NSR + D + AW*
[6]	cIRDD (Cl)	RD_{c-Cl}	*PI*	coarse	Rockrose	RD_{f-Cl}
[7]	fIRDD (Sr)	RD_{f-Sr}	*PI*	fine	Rosemary	*E + NSR + E:NSR + D + AW*
[8]	cIRDD (Sr)	RD_{c-Sr}	*PI*	coarse	Rosemary	RD_{f-Sr}

Two models, fIRDD+m and cIRDD+m ([1] and [2] in Table 1), tested exclusively the performance of the two identification methods used, microsatellite analysis and plant injection. These models were fitted only for rosemary plants, as this was the only species which roots were identified using both methods. Only the rosemary individuals for which at least one root fragment was linked to a reference individual were considered, removing all plants for which no positive result was obtained (seven out of fourteen individuals in plot 1, clustering six out of eight genotypes, were removed). Additionally, we only accounted for the diameter class S for the fine roots model, as those were the only identified using DNA analysis. Therefore, in these two models, we were only interested in the effect and p-value of the factor *m* (method used).

We fitted six more models ([3] to [8] in Table 1)—one fIRDD and one cIRDD for each one of the three focal species—aiming at obtaining biological information about the plants foraging strategies and root system size. For such models, we used the data from plant injection method exclusively, as it proved to be more efficient overall and because we obtained information for a larger range of root diameters. For the fIRDD models, we accounted for all roots with diameter < 2 mm. We predicted the number of roots from the XXS class linked to plant individuals based in the total number of roots of such diameter class in the soil

sample and the proportion of roots of the XS diameter class linked to the same individual in the sample. We performed a backwards stepwise model selection, and non-significant variables at a 95% confidence level were removed at each step. We will discuss the specific results of these fIRDD models and their implications at the level or the root foraging behavior ecology and competition among plants in a different publication (*in prep.*).

For the purpose of this publication, we use these models' predictions to obtain individual-level information to establish allometries for each species, and assess which plant metric is a better allometric predictor. We integrated all the predicted root densities across soil space, accounting for the mean percentage of rooting volume in each plot, to obtain the total root biomass of each plant. Using this plant-level information, we established several allometric relations for each shrub species in the study, assuming they all followed power laws of the form $Y = \alpha X^{\beta}$ (Niklas, 2004). As predictive variables (X) we used both the stem diameter at the ground level and the biovolume of the plant. As response variables (Y) we used biomass measures from aboveground (Total aboveground, Photosynthetic, Photosynthetic labile, Structural labile, and Reproductive, labile referring to turnover of biomass recovered in litter traps), areas measured from the stem cut (Hardwood, Sapwood), and biomass measures from belowground (Total belowground, Fine roots). Such allometries were established by fitting linear equations to log-log transformed data. For each case, we calculated the Pearson's correlation between log-transformed variables and the t-distribution significance tests for Pearson's correlation (Hollander, Wolfe, & Chicken, 2003). We tested for classic, functional (physiologically active tissues), and dynamic (rates, per year) allometries. We only carried out the latter for two species (gum rockrose and rosemary) for which we had collected reproduction and aboveground tissue turnover data.

3 Results

3.1 Hydraulic model results

The mean and range of values for water potential of each dye color measured are as shown in Fig. 1a.

With these values, we plotted $\vec{v_{10}}(f)$ for the different stem vessel diameters and dye water potentials (Fig. 1b).

3.2 Method comparison IRDD model results

The DNA and dying methods yielded consistent RD's, because there was no significant effect of method on the estimated distributions for either fIRDD+*m* model (*m*, t = 0.770, p = 0.441) or cIRDD+m model (*m*, M t = -0.144, p = 0.889; PI t = -0.201, p = 0.845).

3.3 Allometric relations

Consider two easy-to-measure, non-destructive metrics as potential structural predictors for shrub allometries—the basal diameter (stem diameter at the ground level), and the plant biovolume (the volume

occupied by the plant crown). We show the correlation between these metrics and with shrub age in Fig. 2 **(top left panels**). Biovolume and stem diameter were strongly correlated with each other for all three species. Diameter was positively correlated with plant age for all three species. In contrast, biovolume was weakly or insignificantly correlated with age.

Both biovolume and diameter were significantly correlated with hardwood area and aboveground biomass in all three species. However, diameter was positively correlated with belowground biomass only in gum rockrose while biovolume was correlated with belowground biomass for rockrose and rosemary (Fig. 2). Biovolume and diameter were both positively correlated with sapwood area and photosynthetic material in all species. Both metrics were also significantly correlated with fine root biomass of rockrose, but only biovolume seemed to be a reliable predictor of fine root biomass in rosemary as well (Fig. 3). When analyzing the dynamical carbon allocation, allometries for labile biomass fractions showed significant positive correlation between both the aboveground biovolume and stem diameter with both the wood tissue turnover and reproductive biomass per surface area in the case of rosemary, but biovolume was also a significantly related with reproductive biomass in gum rockrose (Fig. 4). Based on these allometric results, we can conclude that shrub biovolume allowed us to find more significant plant allometries (19, of which four belowground) than stem diameter (16, of which two belowground) across species, and is therefore a better predictor of shrub metrics.

4 Discussion

4.1 Microsatellite vs. plant injection

While coring techniques are diverse and many mechanical systems already exist, most ecological root studies still rely on hand-operated corers. Rotary drilling is a very effective coring technique, yet, like most mechanical coring systems, it involves equipment that is usually expensive, large and heavy (i.e. truck-mounted systems) (Abzalov, 2016), which limits its use in many wild locations. However, more affordable and transportable diamond core drilling machines are widely available because of their use in construction industry to drill reinforced concrete. These machines can fit in most standard-sized cars, and can be transported locally by hand, but can only be operated after being stably fixed to a substrate. By adapting the use of a drilling machine of this type, we were able to successfully extract large soil cores with woody roots in one of the hardest existing soils, a granitic leptosol. When encountering a rock, the machine was able to cut through it and, after extracting a granite column, we were able to continue sampling the soil underneath the rock. Generally, the cores were extracted over a time period ranging from five minutes when no rocks were encountered, to around 30 minutes for the cores containing large rocks.

The comparison between the two identification methods tested—microsatellite analysis and plant injection with dyes—demonstrates that the use of plant injection with dyes is the least restrictive and most cost-effective of the two. Microsatellite analysis is restricted because of the limited availability of species-specific microsatellite markers. The relative costs of linking roots was two orders of magnitude larger using microsatellite analysis (~$400 per linked root) than dye injection (~$4 per linked root). Of all

the analyzed roots, proportionally more root fragments were successfully linked to a plant using dye injection (~25%) than microsatellite analysis (~16%) (Fig. 5, **central**), even though 14 plants in the microsatellite-analyzed plots were sampled for aboveground reference (representing roughly all plants in the plot's surroundings) yet only between one and five plants were injected in the other plots (limited by the number of different colors used). The two different methods results supported one another, in that there was no significant effect of method on estimated RDs in the IRDD+*m* models. Even so, this result does not deny that microsatellite was overall less effective as only the plants with at least one root identified were included in the model (see section 2.5): This result indicates that microsatellite yielded results comparable to plant injection for the plant individuals for which it worked well, but failed totally for some of the sampled individuals.

Plant injection also produces the lowest degree of uncertainty for estimates of IRDD. Indeed, an important distinction between the two methods is that the microsatellite analyses cannot distinguish physically separate individuals with the same or similar genotype. These could be ramets, or alternatively separate individuals that the selected loci were not able to discern. Indeed, seven of the 14 plants we analyzed with the DNA method were assigned to two genotypes (Fig. 5, **left panel**). Also, while both methods are subject to errors in negative results (some of the roots that were not linked to any plant might actually belong to one of the focal plants), errors in positive results are likely to occur only using the microsatellite method. In addition, plant injection has other strengths such as allowing the measurement of sapwood area, and the capacity to uncover unambiguous connections between individuals that appear separate above ground, but are connected belowground, because the dye is transported to all the living tissues of the physiological individual, including the leaves in the non-cut branches, where it can be seen with the naked eye.

When comparing the different techniques used to identify the dye in root fragments, we see that the visual identification was more successful than dissolution in water baths. This is especially true for wide root diameters, because the proportion of successful detections shifts toward water baths for roots with smaller diameters. We also observed that cool colors (blue, green), which are difficult to confuse with natural wood colors, produce more visual detections than warm colors. However, for warm colors (red, purple, yellow) the dissolution identification technique was proportionally more successful. Our results also suggest that the optimal time for dye dissolution is two hours, at which time we observe a peak in the fraction detected. Five minutes is not enough time for the dye to dissolve in the warm water, while 24 hours proved to be too long (Fig. 5, **right panel**). After 24 hours, most new identifications appeared to be yellow, and we suspect that the water may have been stained in yellowish-brownish colors from the infusion of the natural plant materials after so much time soaking. This yellow color could have been misidentified as yellow or warm dyes, resulting in a potential source of error in positive results after 24 hours of dissolution.

One important avenue for future research would be to experiment with different kinds of dyes and other chemical tags. For example, a dye that fluoresces at a specific wavelength could allow the presence of

dye to be detected by an electronic sensor at concentrations that would have been invisible to the naked eye.

4.2 Biovolume vs. stem diameter at the ground level

Published shrub allometric relations have been based on the stem basal diameter (at the ground level) (Allen et al., 2008), the stem diameter at 15 cm height (He et al., 2018), and stem apparent volume (Usó et al., 1997). All these measures can be problematic, because shrubs are typically multistem, and often start ramifying very close to ground level, or even sometimes belowground, and other studies rely on the measurement of several stems per plant (Matula, Damborská, Nečasová, Geršl, & Šrámek, 2015). On the other hand, the total plant height and crown area (or crown diameter) are non-destructive measures that are easy to collect for most shrub species. Researchers can obtain an estimate of total aboveground plant biovolume by assuming different canopy shapes, and some studies have used biovolume as a base for shrub allometric relations (Ruiz-Peinado, Moreno, Juarez, Montero, & Roig, 2013; Chibani et al., 2021).

For our study, we collected measurements of the basal diameter of the stem, and also estimated the plant biovolume. We observed that, while both metrics were correlated with each other, they had surprisingly dissimilar ability to predict other quantities. We detected a significant relationship between the age of plants and the stem basal diameter (and hardwood basal area) for all species. This was expected, because the stem grows annually as the plant does, creating new hardwood rings every growing season (Zimowski, Leuschner, Gärtner, & Bergmeier, 2014). Biovolume did not scale with the age of the plants, yet it was a better predictor of the other dependent biometric variables. Indeed, the general size of shrub plants may not scale well with their ages, because multi-stem woody plants can lose whole stems in especially stressful years, a strategy recognized as beneficial for survival in drylands (Tanentzap, Mountford, Cooke, & Coomes, 2012; Götmark, Götmark, & Jensen, 2016). Losing a stem implies reducing plant biovolume together with all the associated above- and belowground biomass, but not the stem basal diameter (when this is below the stem insertion). Indeed, our results indicate that stem basal diameter may be a good proxy for shrub age, but, because shrubs' size can grow in good years but shrink in stressful years, biovolume seems to be a better predictor of general plant biometry.

Declarations

Statements and Declarations

This work was funded by Princeton University's High Meadows Environmental Institute-Carbon Mitigation Initiative (HMEI-CMI). CC acknowledges funding from The May Fellowship in the Department of Ecology and Evolutionary Biology, Princeton University. The authors have no relevant financial or non-financial interests to disclose. CC and SWP conceived the ideas; CC, JV, FV, and SWP designed methodology; CC, LRT, NMM, AV and AMB collected the data; CC analyzed the data; CC and NMM led the writing of the manuscript; FV and SWP funded this study; all authors contributed critically to the drafts and gave final

approval for publication. The datasets generated during and analyzed during the current study are available as an electronic supplementary material.

Acknowledgments

We are very grateful to the *Ayuntamiento de Candeleda* for allowing us to work in their municipal properties at *Las Tejoneras*. Many thanks to Hannes De Deurwaeder for critical reading of the manuscript. Thanks to Ismael Aranda for sharing with us research materials and equipment. Thanks to David López Quiroga for processing and scanning the plant stems. Thanks to Kristina K. Corvin for reviewing the English.

References

1. Abzalov, M. (2016). Drilling techniques and drill holes logging. In *Applied mining geology. Modern approaches in solid earth sciences* (12th ed., pp. 39–77). Cham: Springer. doi:10.1007/978-3-319-39264-6_4
2. Addo-Danso, S. D., Prescott, C. E., & Smith, A. R. (2016). Methods for estimating root biomass and production in forest and woodland ecosystem carbon studies: A review. *Forest Ecology and Management*, *359*, 332–351. doi:10.1016/j.foreco.2015.08.015
3. Allen, A. P., Pockman, W. T., Restrepo, C., & Milne, B. T. (2008). Allometry, growth and population regulation of the desert shrub Larrea tridentata. *Functional Ecology*, *22*(2), 197–204. doi:10.1111/j.1365-2435.2007.01376.x
4. Bardgett, R. D., Mommer, L., & De Vries, F. T. (2014). Going underground: Root traits as drivers of ecosystem processes. *Trends in Ecology and Evolution*, *29*(12), 692–699. doi:10.1016/j.tree.2014.10.006
5. Brunner, I., Brodbeck, S., Büchler, U., & Sperisen, C. (2001). Molecular identification of fine roots of trees from the Alps: Reliable and fast DNA extraction and PCR-RFLP analyses of plastid DNA. *Molecular Ecology*, *10*(8), 2079–2087. doi:10.1046/j.1365-294X.2001.01325.x
6. Cabal, C., Deurwaerder, H. De, & Matesanz, S. (2021). Field methods to study the spatial root density distribution of individual plants. *Plant and Soil*, *462*, 25–46. doi:doi.org/10.1007/s11104-021-04841-z
7. Cabal, C., Martínez-García, R., De Castro Aguilar, A., Valladares, F., & Pacala, S. W. (2020). The Exploitative Segregation of Plant Roots. *Science*, *370*(6521), 1197–1199. doi:10.1126/science.aba9877
8. Cahill, J. F., McNickle, G. G., Haag, J. J., Lamb, E. G., Nyanumba, S. M., & Clair, C. C. S. (2010). Plants integrate information about nutrients and neighbors. *Science*, *328*(5986), 1657. doi:10.1126/science.1189736

9. Chen, G., Hobbie, S. E., Reich, P. B., Yang, Y., & Robinson, D. (2019). Allometry of fine roots in forest ecosystems. *Ecology Letters*, *22*(2), 322–331. doi:10.1111/ele.13193
10. Chibani, R., Tlili, A., Salem, F. Ben, Louhaichi, M., Belgacem, A. O., & Neffati, M. (2021). Assessment of long-term protection on the aboveground biomass and organic carbon content using two non-destructive techniques: case of the Sidi Toui National Park in southern Tunisia. *African Journal of Range & Forage Science*, 1–11. doi:10.2989/10220119.2021.1928752
11. Drexhage, M., & Colin, F. (2001). Estimating root system biomass from breast-height diameters. *Forestry*, *74*(5), 491–497. doi:10.1093/forestry/74.5.491
12. Eldridge, D. J., Bowker, M. A., Maestre, F. T., Roger, E., Reynolds, J. F., & Whitford, W. G. (2011). Impacts of shrub encroachment on ecosystem structure and functioning: Towards a global synthesis. *Ecology Letters*, *14*(7), 709–722. doi:10.1111/j.1461-0248.2011.01630.x
13. Elzein, T. M., Blarquez, O., Gauthier, O., & Carcaillet, C. (2011). Allometric equations for biomass assessment of subalpine dwarf shrubs. *Alpine Botany*, *121*(2), 129–134. doi:10.1007/s00035-011-0095-3
14. Fischer, F. J., Maréchaux, I., & Chave, J. (2019). Improving plant allometry by fusing forest models and remote sensing. *New Phytologist*, *223*(3), 1159–1165. doi:10.1111/nph.15810
15. Freschet, G. T., Pagès, L., Iversen, C. M., Comas, L. H., Rewald, B., Roumet, C., … McCormack, M. L. (2021). A starting guide to root ecology: strengthening ecological concepts and standardising root classification, sampling, processing and trait measurements. *New Phytologist*, *232*(3), 973–1122. doi:10.1111/nph.17572
16. Freschet, G. T., Roumet, C., Comas, L. H., Weemstra, M., Bengough, A. G., Rewald, B., … Stokes, A. (2021). Root traits as drivers of plant and ecosystem functioning: current understanding, pitfalls and future research needs. *New Phytologist*, *232*(3), 1123–1158. doi:10.1111/nph.17072
17. Fusco, E. J., Rau, B. M., Falkowski, M., Filippelli, S., & Bradley, B. A. (2019). Accounting for aboveground carbon storage in shrubland and woodland ecosystems in the Great Basin. *Ecosphere*, *10*(8). doi:10.1002/ecs2.2821
18. Götmark, F., Götmark, E., & Jensen, A. M. (2016). Why be a shrub? A basic model and hypotheses for the adaptive values of a common growth form. *Frontiers in Plant Science*, *7*(JULY2016), 1–14. doi:10.3389/fpls.2016.01095
19. Hamilton, G. J. (1975). *Forest mensuration handbook*. (F. Commission, Ed.). London: HMSO books.
20. He, A., McDermid, G. J., Rahman, M. M., Strack, M., Saraswati, S., & Xu, B. (2018). Developing allometric equations for estimating shrub biomass in a boreal fen. *Forests*, *9*(9), 1–14. doi:10.3390/f9090569
21. Hollander, M., Wolfe, D. A., & Chicken, E. (2003). *Nonparametric Statistical Methods* (3rd ed.). New York, US: John Wiley & Sons.
22. Huang, J., Zhang, G., Zhang, Y., Guan, X., Wei, Y., & Guo, R. (2020). Global desertification vulnerability to climate change and human activities. *Land Degradation and Development*, *31*(11), 1380–1391. doi:10.1002/ldr.3556

23. Jones, F. A., Erickson, D. L., Bernal, M. A., Bermingham, E., Kress, W. J., Herre, E. A., … Turner, B. L. (2011). The roots of diversity: Below ground species richness and rooting distributions in a tropical forest revealed by DNA barcodes and inverse modeling. *PLoS ONE*, *6*(9), 1-10 e24506. doi:10.1371/journal.pone.0024506
24. Kemper, J., Cowling, R. M., & Richardson, D. M. (1999). Fragmentation of South African renosterveld shrublands: Effects on plant community structure and conservation implications. *Biological Conservation*, *90*(2), 103–111. doi:10.1016/S0006-3207(99)00021-X
25. Kirkham, M. B. (2014). *Principles of soil and plant water relations* (2nd ed.). Oxford, UK.: Elsevier.
26. Lal, R. (2004). Carbon sequestration in dryland ecosystems. *Environmental Management*, *33*(4), 528–544. doi:10.1007/s00267-003-9110-9
27. Lambers HFS, Chapin III FS, Pons TL (2008) Plant physiological ecology, Second. Springer, New York, US
28. Lang, C., Dolynska, A., Finkeldey, R., & Polle, A. (2010). Are beech (Fagus sylvatica) roots territorial? *Forest Ecology and Management*, *260*(7), 1212–1217. doi:10.1016/j.foreco.2010.07.014
29. Lux, A., & Rost, T. L. (2012). Plant root research: the past, the present and the future. *Annals of Botany*, *110*(2), 201–204. doi:10.1093/aob/mcs156
30. Ma, X. zhong, & Wang, X. ping. (2021). Aboveground and belowground biomass and its' allometry for Salsola passerina shrub in degraded steppe desert in Northwestern China. *Land Degradation and Development*, *32*(2), 714–722. doi:10.1002/ldr.3772
31. Maestre, F. T., Benito, B. M., Berdugo, M., Concostrina-Zubiri, L., Delgado-Baquerizo, M., Eldridge, D. J., … Soliveres, S. (2021). *Biogeography of global drylands*. *New Phytologist*. doi:10.1111/nph.17395
32. Matula, R., Damborská, L., Nečasová, M., Geršl, M., & Šrámek, M. (2015). Measuring biomass and carbon stock in resprouting woody plants. *PLoS ONE*, *10*(2), 12–15. doi:10.1371/journal.pone.0118388
33. Murakami, T., Shimano, S., Kaneda, S., Nakajima, M., Urashima, Y., & Miyoshi, N. (2006). Multicolor staining of root systems in pot culture. *Soil Science and Plant Nutrition*, *52*(5), 618–622. doi:10.1111/j.1747-0765.2006.00078.x
34. Murakami, T., Shimano, S., Kaneda, S., Nakajima, M., Urashima, Y., & Miyoshi, N. (2011). Improvement of root staining method for field applications. *Soil Science and Plant Nutrition*, *57*(4), 541–548. doi:10.1080/00380768.2011.590945
35. Muukkonen, P. (2007). Generalized allometric volume and biomass equations for some tree species in Europe. *European Journal of Forest Research*, *126*(2), 157–166. doi:10.1007/s10342-007-0168-4
36. O'Brien, S. T., Hubbell, S. P., Spiro, P., Condit, R., Robin, B., Hubbell, S. P., & Spiro, P. (1995). Diameter , Height , Crown , and Age Relationship in Eight Neotropical Tree Species. *Ecology*, *76*(6), 1926–1939. doi:10.2307/1940724
37. Poorter, H., Fiorani, F., Pieruschka, R., Wojciechowski, T., van der Putten, W. H., Kleyer, M., … Postma, J. (2016). Pampered inside, pestered outside? Differences and similarities between plants growing in controlled conditions and in the field. *New Phytologist*, *212*(4), 838–855. doi:10.1111/nph.14243

38. R Core Team. (2017). R: A language and environment for statistical computing. Vienna, Austria: R Foundation for Statistical Computing. Retrieved from https://www.r-project.org/
39. Rivas-Matínez, S., & Armaiz, C. (1984). Bioclimatologia Y Vegetacion en la Península Ibérica. *Bulletin de La Société Botanique de France. Actualités Botaniques*, *5*, 110–120. doi:10.1080/01811789.1984.10826653
40. Ruiz-Peinado, R., Moreno, G., Juarez, E., Montero, G., & Roig, S. (2013). The contribution of two common shrub species to aboveground and belowground carbon stock in Iberian dehesas. *Journal of Arid Environments*, *91*, 22–30. doi:10.1016/j.jaridenv.2012.11.002
41. Saari, S. K., Campbell, C. D., Russell, J., Alexander, I. J., & Anderson, I. C. (2005). Pine microsatellite markers allow roots and ectomycorrhizas to be linked to individual trees. *New Phytologist*, *165*(1), 295–304. doi:10.1111/j.1469-8137.2004.01213.x
42. Schenk, H. J., & Jackson, R. B. (2002). Rooting depths, lateral root spreads and below-ground/ above-ground allometries of plants in water-limited ecosystems. *Journal of Ecology*, *90*, 480–494. doi:10.1046/j.1365-2745.2002.00682.x
43. Schrader-Patton, C. C., & Underwood, E. C. (2021). New biomass estimates for chaparral-dominated southern California landscapes. *Remote Sensing*, *13*(8), 1–24. doi:10.3390/rs13081581
44. Segarra-Moragues, J. G., & Gleiser, G. (2009). Isolation and characterisation of di and tri nucleotide microsatellite loci in Rosmarinus officinalis (Lamiaceae), using enriched genomic libraries. *Conservation Genetics*, *10*(3), 571–575. doi:10.1007/s10592-008-9572-7
45. Smith, B. W., & Brand, G. J. (1983). Allometric biomass equations for 98 species of herbs, shrubs, and small trees. *St. Paul, MN: US Dept. of Agriculture, Forest Service, North Central Forest Experiment Station*, *Research N*, 1–8.
46. Tanentzap, A. J., Mountford, E. P., Cooke, A. S., & Coomes, D. A. (2012). The more stems the merrier: Advantages of multi-stemmed architecture for the demography of understorey trees in a temperate broadleaf woodland. *Journal of Ecology*, *100*(1), 171–183. doi:10.1111/j.1365-2745.2011.01879.x
47. Tomaselli, R. (1977). The Degradation of the Mediterranean Maquis. *Ambio*, *6*(6), 356–362. Retrieved from http://www.jstor.org/stable/4312322
48. Tyree, M. T., & Ewers, F. W. (1991). The hydraulic architecture of trees and other woody plants. *New Phytologist*, *119*(3), 345–360. doi:10.1111/j.1469-8137.1991.tb00035.x
49. Usó, J. L., Mateu, J., Karjalainen, T., & Salvador, P. (1997). Allometric regression equations to determine aerial biomasses of Mediterranean shrubs. *Plant Ecology*, *132*(1), 59–69. doi:10.1023/A:1009765825024
50. Wirth, C., Schumacher, J., & Schulze, E. D. (2004). Generic biomass functions for Norway spruce in Central Europe - A meta-analysis approach toward prediction and uncertainty estimation. *Tree Physiology*, *24*(2), 121–139. doi:10.1093/treephys/24.2.121
51. Wullschleger, S. D., Epstein, H. E., Box, E. O., Euskirchen, E. S., Goswami, S., Iversen, C. M., … Xu, X. (2014). Plant functional types in Earth system models: Past experiences and future directions for

application of dynamic vegetation models in high-latitude ecosystems. *Annals of Botany*, *114*(1), 1–16. doi:10.1093/aob/mcu077

52. Zimowski, M., Leuschner, H. H., Gärtner, H., & Bergmeier, E. (2014). Age and diversity of Mediterranean dwarf shrublands: A dendrochronological approach along an altitudinal gradient on Crete. *Journal of Vegetation Science*, *25*(1), 122–134. doi:10.1111/jvs.12067

Figures

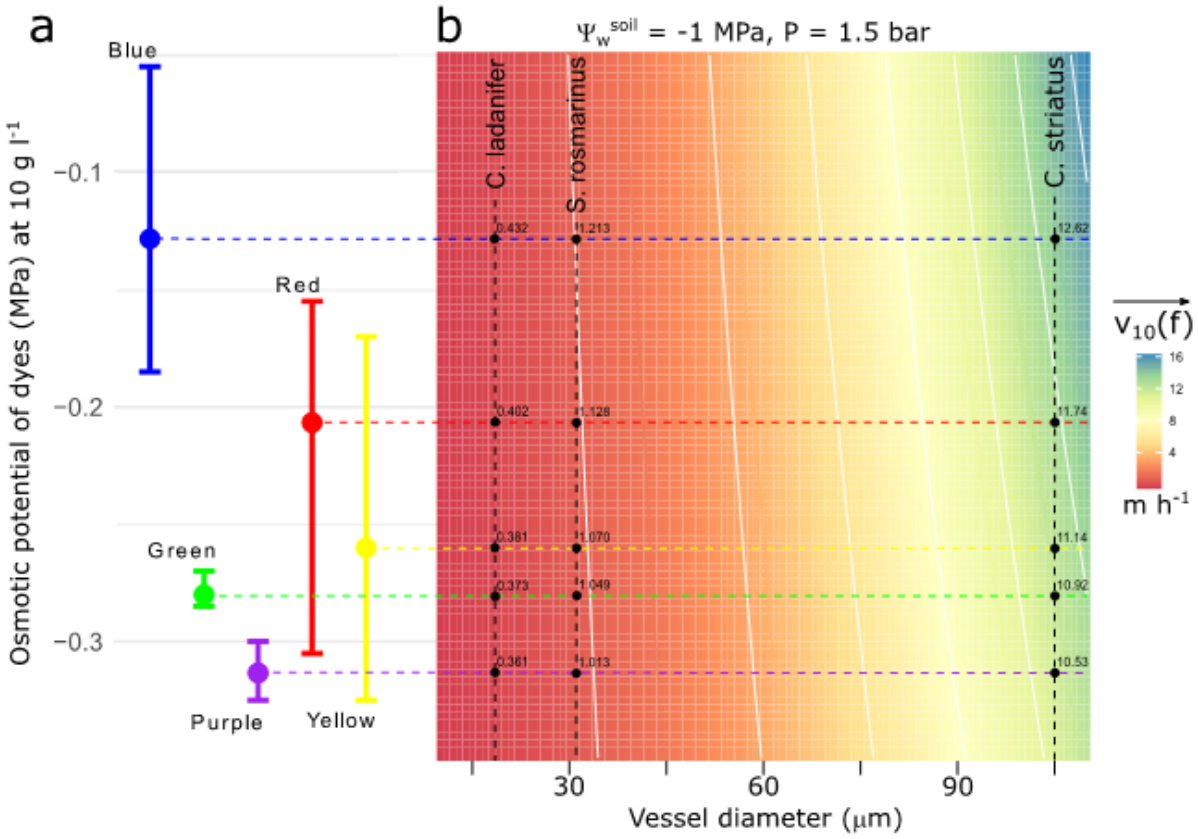

Figure 1: Model results used to estimate pressure exertion time for plant injection at P = 1.5 bar and Ψ_w^{soil} = -1 MPa. **a**- Means and range of values of the osmotic potential for the different color dyes injected to plants. **b**- Contour plot for $\overrightarrow{v_{10}(f)}$, indicating the value for all the combinations of dye colors and focal species' vessel diameters.

Figure 1

See image above for figure legend

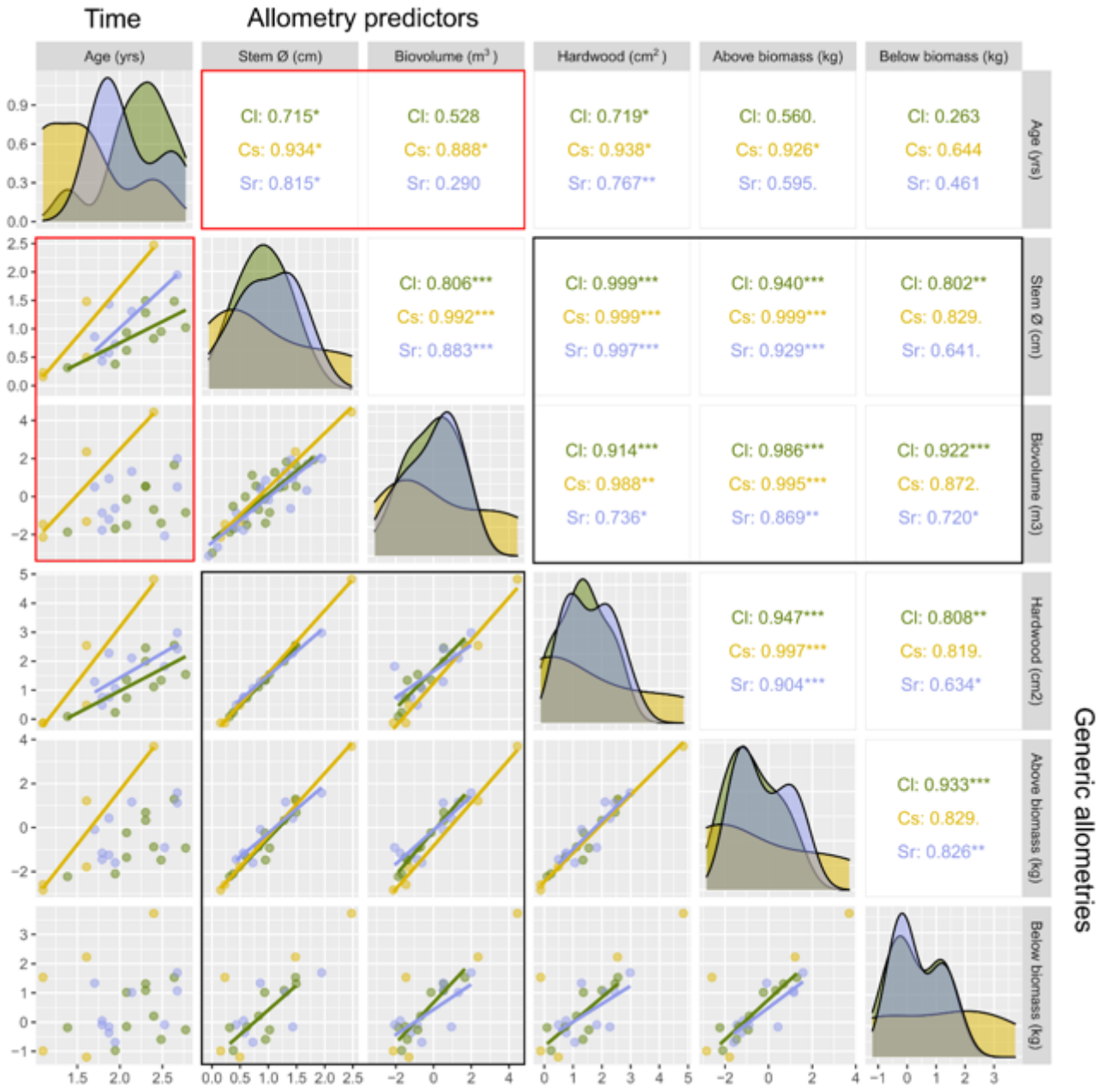

Figure 2

Allometric relations between shrub age and two architectural predictors: stem diameter and biovolume (red boxes); and between architectural predictors and three general allometric estimates: hardwood, aboveground biomass, and belowground biomass (black boxes). All allometric relations correspond to power laws (i.e., all variables are log-transformed). Upper plots show Pearson's R and significance with significance codes for p being '***' 10-3, '**' 10-2, '*' 0.05, '·' 0.1, and ' ' 1. Diagonal plots are data distributions. Lower plots are data scatterplots, lines shown when correlation was significant at a confidence level of 0.05. Cl = rockrose, *C. ladanifer*, Cs = broom, *C. striatus*; and Sr = rosemary, *S. rosmarinus*.

Figure 3

Allometric relations between shrub architectural predictors and three functional variables (black boxes): sapwood (active transport of water), photosynthetic material (active transpiration), and fine roots (active water absorption). All allometric relations correspond to power laws (i.e., all variables are log-transformed). Upper plots show Pearson's R and significance with significance codes for p being '***' 10^{-3}, '**' 10^{-2}, '*' 0.05, '·' 0.1, and ' ' 1. Diagonal plots are data distributions. Lower plots are data scatterplots, lines shown when correlation was significant at a confidence level of 0.05. Cl = rockrose, *C. ladanifer*, Cs = broom, *C. striatus*; and Sr = rosemary, *S. rosmarinus*.

Figure 4

Dynamic (per year rates) allometric relations between shrub architectural predictors and variables of labile biomass fractions (black boxes): leaves (photosynthetic), wood (non-photosynthetic), and reproduction material, shed by plants per surface area unit and per year. All allometric relations correspond to power laws (i.e., all variables are log-transformed). Upper plots show Pearson's R and significance with significance codes for p being '***' 10^{-3}, '**' 10^{-2}, '*' 0.05, '·' 0.1, and ' ' 1. Diagonal plots are data distributions. Lower plots are data scatterplots, lines shown when correlation was significant at a confidence level of 0.05. Cl = rockrose, *C. ladanifer*, Cs = broom, *C. striatus*; and Sr = rosemary, *S. rosmarinus*.

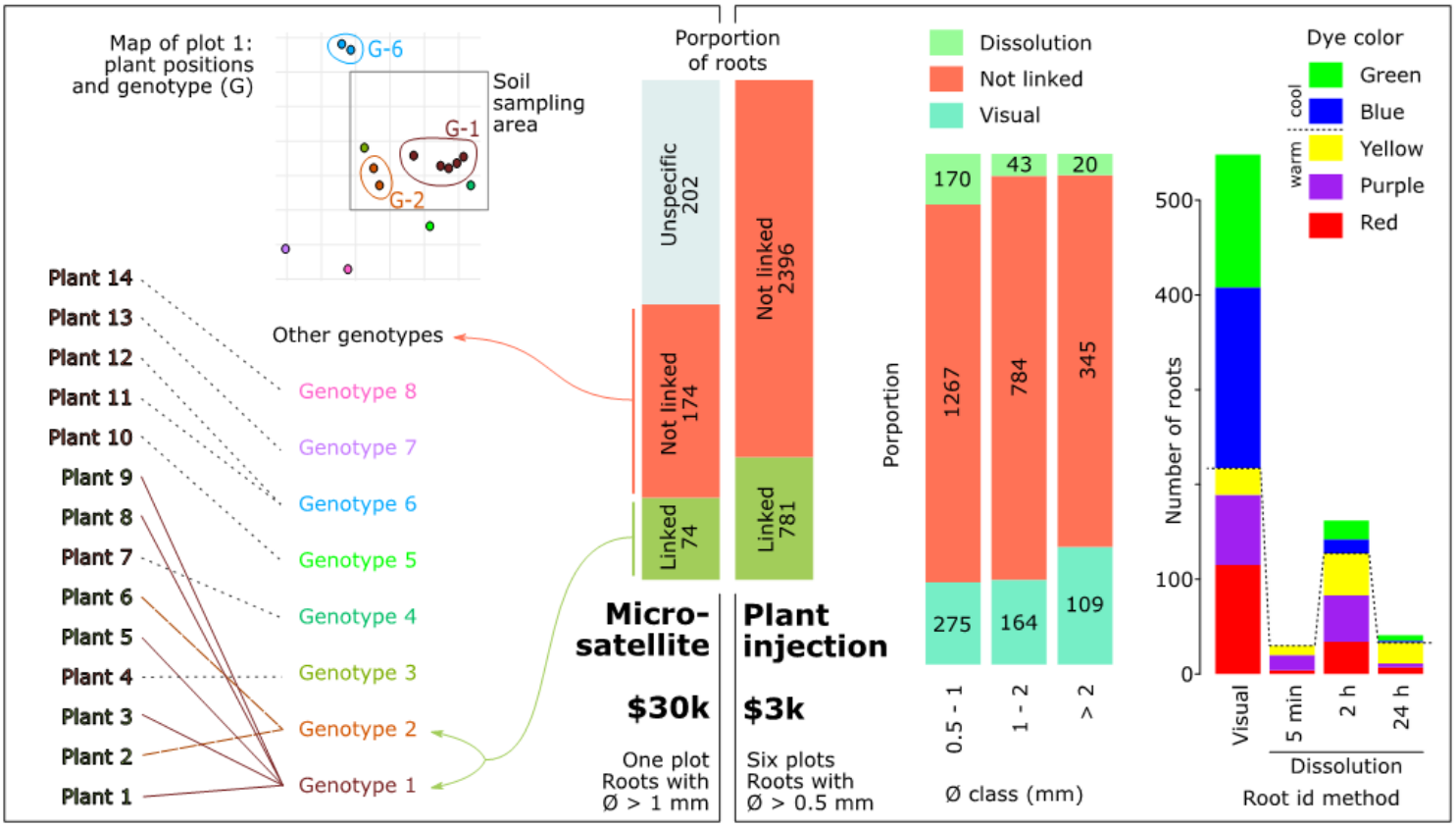

Figure 5

Summary of results from linking root fragments to plant individuals using two identification methods: Microsatellite (left) and plant injection with dyes (right). Central bar plots represent the proportion of analyzed roots successfully linked or not linked to plants. “Unspecific” results account for roots for which PCR/barcoding results were negative, non-specific, or roots that were associated with a different species (not rosemary). The left panel shows how different roots and plants analyzed with microsatellite analyses were linked to several genotypes (bottom), and how plants were spatially grouped by genotypes (top). The right panel shows the proportional performance of the visual and the dissolution identification methods per root diameter class, and the number of roots per color used successfully linked using the different identification techniques (visual and different dissolution times)

Supplementary Files

This is a list of supplementary files associated with this preprint. Click to download.

- SMAMethodforIdentifyingShrubIRDDpreview.mp4
- SMDetailedmaterialsandmethods.pdf